09:15:16 OCA PAD AMENDMENT - PROJECT HEADER INFORMATION 02/03/93

Active

Project #: C-50-615 Cost share #: Rev #: 1
Center # : 10/24-6-R7430-0A0 Center shr #: OCA file #:
Work type : RES
Contract#: SUBCONT DTD 12/15/88 Mod #: BR DTD 1/26/93 Document : OTH
Prime #: Contract entity: GTRC

Subprojects ? : N CFDA:
Main project #: PE #: N/A

Project unit: GVU Unit code: 02.010.314
Project director(s):
EZQUERRA N F ESML (404)894-7029

Sponsor/division names: EMORY UNIVERSITY / ATLANTA, GA
Sponsor/division codes: 400 / 012

Award period: 911201 to 921130 (performance) 930115 (reports)

Sponsor amount	New this change	Total to date
Contract value	10,531.85	82,594.85
Funded	10,531.85	82,594.85
Cost sharing amount		0.00

Does subcontracting plan apply ?: N

Title: UNIFIED APPROACH TO QUANTIFY AND VISUALIZE CARDIAC IMAGERY

PROJECT ADMINISTRATION DATA

OCA contact: Kathleen R. Ehlinger 894-4820

Sponsor technical contact

DR. ERNEST V. GARCIA
(000)000-0000

ASSOCIATE PROFESSOR OF RADIOLOGY
EMORY UNIVERSITY
1364 CLIFTON ROAD, NE
ATLANTA, GA 30322

Sponsor issuing office

DR. ANN R. STEVENS
(404)727-2503

ASSOC. VP ACADEMIC AFFAIRS AND
RESEARCH/DIR. OF SPONSORED PROGRAMS
303 B, SCHOOL OF DENTISTRY
ATLANTA, GA 30322

Security class (U,C,S,TS) : U ONR resident rep. is ACO (Y/N): N
Defense priority rating : N/A NIH supplemental sheet
Equipment title vests with: Sponsor X GIT
NONE PROPOSED.
Administrative comments -
ISSUED TO CARRY FORWARD UNEXPENDED FUNDS FROM PRIOR YEAR - C-50-611.

GEORGIA INSTITUTE OF TECHNOLOGY
OFFICE OF CONTRACT ADMINISTRATION

NOTICE OF PROJECT CLOSEOUT

Closeout Notice Date 01/18/94

Project No. C-50-615 Center No. 10/24-6-R7430-0A0

Project Director EZQUERRA N F School/Lab GVU

Sponsor EMORY UNIVERSITY/ATLANTA, GA

Contract/Grant No. SUBCONT DTD 12/15/88 Contract Entity GTRC

Prime Contract No.

Title UNIFIED APPROACH TO QUANTIFY AND VISUALIZE CARDIAC IMAGERY

Effective Completion Date 921130 (Performance) 930115 (Reports)

Closeout Actions Required:	Y/N	Date Submitted
Final Invoice or Copy of Final Invoice	Y	930917
Final Report of Inventions and/or Subcontracts	Y	
Government Property Inventory & Related Certificate	N	
Classified Material Certificate	N	
Release and Assignment	N	
Other	N	

Comments

Subproject Under Main Project No.

Continues Project No. C-50-611

Distribution Required:

Project Director	Y
Administrative Network Representative	Y
GTRI Accounting/Grants and Contracts	Y
Procurement/Supply Services	Y
Research Property Managment	Y
Research Security Services	N
Reports Coordinator (OCA)	Y
GTRC	Y
Project File	Y
Other CARL BAXTER-FMD	Y
	N

NOTE: Final Patent Questionnaire sent to PDPI.

SECTION 2. RESEARCH PLAN

A. SPECIFIC AIMS

The long-term objectives of the proposed research in this competing continuation application are to continue to develop and validate computer-based methods to multi-dimensionally (≥3) quantify, unify and visualize the coronary arterial tree and the independently acquired distributions of myocardial perfusion and thickening. This will result in a quantitative approach which unifies the anatomic and physiologic determinants of the extent and severity of jeopardized myocardium. The first overall hypothesis is that since the heart is a three-dimensional (3D) object (that moves), methods which quantify and allow visualization of cardiac distributions in at least 3D are more accurate and offer significant advantages over conventional 2D methods. The second and main overall hypothesis is that the integration of cardiac information from the various imaging modalities are more accurately represented by a unified approach (taking into account all of the available quantitative information which is then visualized in one integrated multi-dimensional display) rather than by conventional approaches. The most widespread conventional approach has been the integration in the mind of a diagnostician or referring physician of the information generated by each of the cardiac imaging modalities.

Since none of the cardiac modalities provide well-validated methods for quantifying and rendering information in 3D, which we would then unify into a single model of the heart, we are required to continue the valuable (although labor-intensive) process of developing and validating the 3D approach for each of those techniques. We will continue to focus our major efforts on proving the unification concept using anatomic information from coronary angiography and physiologic information from perfusion SPECT studies. In addition, we will extend the unification concept to include myocardial thickening information from MRI. The specific aims of this proposed research consists of the following projects.

Project 1. Improvement and automation of our methods for the 4D (3D & time) quantification and visualization of anatomic information from coronary angiographic studies in order to determine the extent and severity of coronary artery disease (CAD). The hypothesis is that representation of the coronary arterial tree in 3 or 4D will lead to improvements in the quantitative and qualitative assessment of the anatomic factors associated with CAD, such as location, shape, length, and cross-sectional area of stenoses.

Project 2. Further development and validation of methods for the 4D quantification, and visualization of physiologic information derived from myocardial tomographic studies of radioactive perfusion tracers (Tl-201 and Tc-99m Sestamibi) in order to determine the extent and severity of jeopardized myocardium. The hypothesis is that representation of the myocardial perfusion distribution in 3D will lead to improvements in the assessment of abnormal myocardium such as the size, location and shape of the abnormality.

Project 3. Further development and validation of methods for the 4D quantification, unification and visualization of myocardial thickening derived from multiple gated SPECT Tc-99m sestamibi and gated MRI studies. The hypothesis is that representation of the resting myocardial thickening distribution in 3D will lead to improvements in the assessment of myocardial viability. A second hypothesis is that unification will provide a more accurate approach to assess how well the size, location, magnitude and phase of myocardial thickening as determined from gated Sestamibi studies will correlate with gated MRI determination of myocardial thickening.

Project 4. Further development of methods for the unified quantification and visualization of anatomic and physiologic information in 4D. This will be accomplished through registration and graphical display of angiographic information and myocardial perfusion, and/or thickening information to determine the extent and severity of jeopardized myocardium. The hypothesis is that the unification of the anatomic and physiologic information in 4D will result in a more accurate, quantitative assessment of the amount of jeopardized myocardium. This comprehensive assessment should also lead to improvements in the accuracy of patients' diagnoses, prognosis and selection of therapeutic intervention, since it will be based on a better understanding regarding the degree of dependency (or independence) between these modes of diagnosing CAD and myocardial ischemia/infarction.

Project 5. Further validation and clinical evaluation of the methods proposed in project 4 in experimental animal models and patient studies. We expect this approach to lead to both improved quantification and reduced interobserver variation, thereby promoting more accurate and reproducible interpretation.

B. BACKGROUND AND SIGNIFICANCE

Clinical decisions regarding the diagnosis, prognosis and therapy of a patient with CAD are determined largely by the extent and severity of coronary artery disease and the amount of diseased myocardium which

causes left ventricular (LV) functional impairment (26-37). This assessment is usually based on interpreting anatomic and physiologic information provided by various cardiac imaging modalities. A number of limitations exist at present which jeopardize the accuracy of these interpretations. For instance, although the heart is a 3D object the interpretation is usually made from 2D images (projections or slices). The interpretation is typically made through subjective, visual observation. Moreover, the informational content of the imagery may not be fully exploited, especially if the images corresponding to different modalities are considered separately rather than in a unified manner.

2.B.1 Anatomy: Quantification and visualization of coronary vessel anatomy.

Coronary arteriography remains the "gold standard" for the assessment of the severity and extent of atheromatous obstruction (38). Using contrast injections into the coronary arteries, measurements of the degree of luminal diameter narrowing (both in relative and absolute terms) and the site of the stenoses can be made. This knowledge, coupled with the particular vascular distribution, can be used to quantify the amount of myocardium at jeopardy. Numerous methods for quantifying both of these parameters have been proposed (35,39-42), usually "trading-off" simple, easy-to-implement schemes with more complex and time-consuming schemes that more accurately define disease status.

Visual interpretation of the degree of coronary obstruction has been most commonly employed but has been shown to provide suboptimal intra and interobserver reproducibility (43-46). More importantly, the relative percent diameter stenosis fails to account for the baseline diffuseness of atheromatous obstruction in most patients with CAD (13,25). Thus, measurement of minimal luminal diameter (mean of two orthogonal views) is more likely to provide accurate data on the degree of hemodynamically significant stenoses than measurements of percent diameter.

To date, no scheme has been fully developed to take into account the particular morphology of the stenosis visualized. Recent studies (47-50) have shown that certain morphological features of lesions are important in determining outcome. Irregular lesions that suggest ulceration are more likely to occlude (47) as are lesions which either contain visible thrombus (48), have an abrupt proximal face (49), and/or are markedly eccentric (49). The length and shape of the stenosed segment, and the effect of lesions in series, also need to be taken into account (37,45).

Automated methods. Automated methods have recently been developed and validated (50,51) which use processed biplanar projections to calculate the luminal diameter narrowing from the reconstructed 3D representation of the stenosed vessel. These approaches use edge detection of the coronary vessels in the two projections and reconstruct an elliptical vessel assuming that the two projections are representative of the minor and major axis of the ellipse. If only one projection is available, the background corrected density of the opacified vessel is used to determine the axis perpendicular to the projection. Although many assumptions are associated with these approaches, each with a degree of error, these methods have been shown to have as small as 0.1mm error in measurements of phantoms (52). To date, most of these methods rely on operator-selected identification of stenotic sites and do not offer 3D (or 4D) reconstruction of the entire coronary vascular tree.

Coronary vascular tree reconstructions. Although still in developmental stages, promising semi-automated and automated methods are being proposed (53-59) that use processed biplanar angiographic projections to reconstruct the entire vascular tree usually by triangulation of the 3D position of each object point from the two projections. Although the unique reconstruction of an object usually requires many acquired projections, a point can be uniquely positioned in 3D space if its coordinates are known in two arbitrary (non-parallel) projections. Most of these techniques have in common that they triangulate the vessels' center points paired from the two projections. Once a vessel center point is uniquely determined in 3D space it is given the circular or elliptical dimensions corresponding to the projected vessel diameter in each projection.

These techniques can be divided into five classifications: 1. those that require orthogonal projections (54,55); 2. those that require fixed stereoscopic projections (56,57); 3. those that allow arbitrary orientations but require a separate calibration using a cube phantom with each patient acquisition (53,58); 4. those that allow arbitrary orientations but require knowledge of eight or more object points which can be identified unambiguously in both views (59); and 5. those that allow arbitrary orientations but require knowledge of the relative or absolute orientation of the two radiographic views (1).

Although these methods offer advances in this field they each have limitations. The fixed geometry required by methods 1 and 2 seriously limits their applicability since one of the two biplanar images would usually not be optimal. The additional phantom acquisition with each orientation required by method 3 is cumbersome. The identification of the 8 landmarks by method 4 is not only difficult to automate but also difficult to always identify accurately due to the fact that the landmarks are not points but extended objects

which are seen differently from each of the projections and that the accuracy of the method is sensitive to their exact localization (60). Method 5 at present requires that each angiographic system be carefully calibrated so that the angle and position of the detectors and x-ray tubes are known. Even then, the deformation of the gantry under its own weight leads to reconstruction errors (61). Manufacturers are starting to precalibrate their digital systems to accurately measure and digitally store the parameters required for reconstruction as they become aware of the benefits of 3D angiographic imaging. To date none of these reconstruction techniques have been validated in animal models or patients and thus have not found widespread clinical use.

Many of these methods are limited by extensive operator intervention as well as by the errors associated with reconstructions from two projections. One critical step occurs after each vessel center-point is determined from one of the projections. The algorithm then generates a guideline across the second view which could traverse across several vessels. The reconstruction process is greatly enhanced by the identification of the corresponding vessel. This identification is usually done manually. Recently, a knowledge-based approach for labeling of the vascular network for 3-D reconstruction from biplane projections has been developed which automates this procedure (62).To date, investigators have not attempted to unify anatomic and physiologic information for the assessment of the extent and severity of CAD and the amount of myocardium at jeopardy, as described by the proposed research. Thus, Project 1 is devoted to continue the development, implementation and validation of techniques to generate and quantify 3D patient-specific arterial trees while minimizing or eliminating operator intervention through the application of analytic and knowledge-based techniques.

2.B.2 Physiology: Quantification and visualization of myocardial perfusion. Myocardial perfusion scintigraphy remains the most widespread approach for assessment of the severity and extent of myocardial ischemia and infarction in the clinical setting. Studies have demonstrated that normalization at four hours (or up to 24 hrs) of a Tl-201 stress myocardial perfusion defect is consistent with reversible ischemia (63), whereas lack of manifestation of this reversibility phenomenon is associated with a fixed infarcted myocardial wall (64). Several studies have also demonstrated that Tl-201 stress-delayed imaging is an effective prognostic tool: patients with normal Tl-201 distributions have an excellent prognosis (65), whereas patients with multiple or severe thallium defects have a much higher incidence of untoward cardiac events (66). The main limitation of Tl-201 imaging has been its low photon energy (~80 keV) and its long half-life (73 hrs). Also, it has been suggested that a resting Tl-201 reinjection protocol improves the assessment of myocardial viability (67).

Tc-99m sestamibi has been introduced as a myocardial perfusion tracer (68) with improved imaging characteristics (8) (higher energy - 140 keV and a shorter half-life - 6 hrs) including the potential for multigated tomographic acquisition (69) due to its three-fold increase in count rate compared to Tl-201.

Several studies have suggested that single photon emission computerized tomography (SPECT) offers significant improvement over planar scintigraphy for the detection and localization of myocardial ischemia (71,72) and myocardial infarction, and also that it is better for estimating the extent of myocardial infarction (73,74). Several investigators (75-77) have used extensions of the planar quantification concept to quantify the 3D distribution of myocardial thallium at stress and delayed imaging from SPECT studies. The PI has collaborated in the development of the two most commonly used algorithms based on this approach, developed at Cedars-Sinai (75) and at Emory(77,78). In both approaches, which are similar, the entire myocardium is mapped onto a polar map where the apical tracer distribution appears at the center of a disc and the basal distribution at the periphery (Figure {3.1}3) (Henceforth, the notation Figure {N}n denotes figure n of Appendix N). Both approaches compare the regional thallium distribution to corresponding lower limits of normal distribution to partly compensate for Compton scatter, tissue attenuation and object size effects. Nevertheless, these approaches are still suboptimal for the evaluation of the extent and severity of myocardial ischemia/infarction because this polar mapping: 1) results in significant warping (misrepresentation) of the true 3D distribution, 2) depends on the expertise of the observer in performing "mental" transformations to convert the warped disc (polar map) to a true 3D distribution, and 3) does not account for the regional thickness variations (i.e., true mass) of the myocardium (79).

Thus, Project 2 is devoted to the further development, implementation and validation of techniques to better quantify and visualize true 3D myocardial perfusion distributions.

2.B.3 Physiology: Quantification and visualization of myocardial thickening. Studies in dogs using piezoelectric crystals have shown that myocardial thickening during systole as a percent of end-diastolic thickening is linearly proportional to blood flow (80,81). Echocardiography and magnetic resonance imaging (MRI) have shown that the presence of thickening correlates with other indicators of tissue viability, and thinning correlates with scarring (82-84). Thus measurement of myocardial thickening would permit assessment of perfusion, as well as provide an indicator of myocardial viability. Routine direct measurement

(using endocardial and epicardial edge definition) of myocardial thickness is not accurate with routine gated SPECT (85). Thus, Project 3 is devoted to the development of techniques which use count-based methods of gated SPECT sestamibi images and MRI methods to quantify, visualize and unify true 3D myocardial thickening distributions.

2.B.4. Unified, multidimensional quantification and visualization of coronary anatomy and myocardial distributions of perfusion and thickening. Integration of multiple 3-D imaging modalities into a single composite 3-D display has recently attained attention in neurologic imaging (86,87). Pelizzari et al. (88) have popularized an approach which uses a hill-climbing method to find the linear transformation with the minimum cost between a set of head boundary points obtained by MRI and another set obtained by PET. Clinically, this integrated 3-D model has been shown to depict to surgeons the accurate location of PET-detected metabolic abnormalities with respect to the gyral anatomy visualized with MR (86). Another group has been able to generate a composite 3-D image of cerebral anatomy and vasculature by superimposing angiographic stereo pairs onto volume rendered images of either CT or MR data (87).

In the heart, a method has been reported for the spatial and temporal registration of SPECT and MR images using a modification of the method developed by Pelizzari (89). The method was developed to localize perfusion abnormalities from SPECT in relation to endocardial wall motion and systolic wall thickening from MRI. A rudimentary technique (90) has also been reported that allows the generation of a 3D myocardial surface from a tomographic thallium-201 study, wherein a "generic" normal coronary artery tree was superimposed to provide a familiar anatomical framework for locating perfusion defects. This method, although helpful, is limited by the fact that the coronary tree maps are not patient-specific, and importantly by the fact that thresholded surfaces of the thallium distribution do not represent myocardial perfusion. This largely unexplored unification of coronary vasculature and myocardial physiologic information will continue to be investigated in Project 4.

2.B.5. Uniqueness and Clinical Utility of Research. One of the prominent characteristics of the proposed research is the comprehensive nature of the approach, emphasizing anatomy from coronary arteriography, physiology from myocardial perfusion imaging, and function from imaging myocardial thickening, all in a unified fashion. Another feature of the research is the emphasis placed on both quantification and visualization in 4D of the total amount of myocardium in jeopardy. This innovative approach allows for a more natural, integrated framework for decision-making, thereby helping to establish a methodology for diagnosing, prognosticating and aiding in the selection of therapeutic interventions related to CAD. Moreover, the proposed research will result in an effective tool to assist referring physicians, interventionists and patients in visualizing the true extent of jeopardized and/or necrotic myocardium. This potential for improved visualization is consistent with the recommendation of the NSF advisory panel on the need to fund visualization (91). The unified approach resulting from this research, proposed for coronary arteriography and cardiovascular nuclear imaging in particular, should potentially serve as a model methodology for unification of medical imaging modalities in general.

In addition, the research program is inter-institutional, since it brings together personnel and other resources from two institutions under the auspices of the Emory/Georgia Tech Biotechnology Research Center. This research program has benefited from, and contributed toward, the success of this center. These two institutions will jointly provide to this study the following elements: (a) a vast array of state-of-the-art equipment and facilities consisting of two SPECT systems with multigated tomography capabilities, two angiographic systems with simultaneous digital biplane acquisition, similar computer environments at both institutions and extensive software developed for image processing and analysis (53), geometric modeling (92), and AI software (58); (b) comprehensive clinical information from large data bases of patient studies consisting of tomographic images using Tl-201 or Tc-99m-Sestamibi and MRI and correlative biplane angiographic images; and (c) a team of experienced clinicians, scientists, and researchers.

Importantly, Georgia's General Assembly has recently passed Governor Zell Miller's package in which the State will match $3.75 million from external funds (such as this proposal) to fund eminent scholars, build research facilities and fund equipment. Specifically, in consideration of the scientific, clinical and commercial success of our research team, $450,000 of the above funds has been budgeted in 1992-93 to Drs. Garcia and Ezquerra to purchase state-of-the-art research equipment.

C. PROGRESS REPORT

Personnel who contributed to these investigations:

Emory University

name	title	dates of service	%effort
Ernest Garcia, Ph.D.	Professor, Principal Investigator	12/88-to-date	20*
J. Larry Klein, M.D.	Asst. Professor, Co-Investigator	12/88-11/90 12/90-to-date	10 37
C. David Cooke, MSEE	Computer Scientist	12/88-to-date	60
Spencer King, M.D.	Professor, Co-Investigator	12/88-to-date	5#
E. Gordon DePuey, M.D.	Assoc. Professor, Co-Investigator	12/88-11/90	10#
Gary Roubin, M.D.	Asst. Professor, Co-Investigator	12/88-11/89	5#
Jack Ziffer, M.D.,Ph.D.	Asst. Professor, Co-Investigator	12/90-11/91	5#

Georgia Tech

name	title	dates of service	%effort
Norberto Ezquerra, Ph.D.	Assoc. Professor, Subcontract PI	12/88-to-date	25
John Peifer, MA	Sr. Research Scientist, Co-Investigator	12/88-11/90 12/90-to-date	50 33

*All efforts listed are those recommended by Study Section. Actual funded efforts were modified according to year-to-year cuts (downward-negotiations) as described below.
No salary support requested

Funding History: This continuation proposal is written after 3 years of funding. The table below shows the significant cuts ("downward negotiations") due to NIH budgeting problems which reflects changes in efforts and all funding for the project. Another important consideration is that the direct costs reported includes the indirect cost of the subcontract. The actual direct costs column shows the funds used for this project. Although we are proud of the remarkable progress made (as described below) with such limited funding, clearly the significant cuts made had an impact on our expected productivity and milestones.

	Direct Costs			Indirect Costs	Direct Costs
Year	Recommended	Funded	% cut	(Subcontract)	Actual
01	$166,693	$150,024	10%	$33,532	$116,492
02	$179,161	$145,110	19%	$32,526	$112,584
03	$201,229	$164,825	18%	$26,764	$138,061
04	$209,599	$167,695	20%	$27,442	$140,253

C.2 Summary of Accomplishments:

C.2.1 Specific aims of previous application. To develop and validate computer algorithms for:
Project 1. reconstructing and generating quantitative, patient-specific, 3D arterial maps obtained from coronary angiography,
Project 2. generating 3D quantitative, myocardial perfusion distributions obtained from perfusion tracers,
Project 3. registering, quantifying and visualizing in 3D a unified model of the coronary tree superimposed on the myocardial perfusion distribution.

C.2.2 Progress towards their achievement.
Inventions: Although no patent has been sought, these developments have resulted in parts of 3 copyrighted software packages which have been commercialized thus being made available to the entire field. See descriptions below.
Project 1. Significant progress has been made towards all phases of the development of methodology for the 3-D reconstruction of the coronary vasculature from arbitrary, non-orthogonal biplane angiographic projections using non-parallel geometry. The phases are: 1) image acquisition and correction, 2) structure detection and labeling in each view, 3) the reconstruction process, 4) the 3-D representation (visualization) and 5) validation. Two publications (1,2) describe the achievements of these phases.

1) A Philips (simultaneous) biplane digital angiographic system was carefully calibrated by us to provide accurate readings of the absolute position, for each detector, of the image intensifier tube screen in terms of distance from the isocenter and from the x-ray source as well as the RAO or LAO angulation and the cranial or caudal angulation (rotation and skew angles). A well-known algorithm was implemented to correct for the pin-cushion distortion which is caused by the slight curvature of the image intensifier screen (53).

2) Two automatic edge detection algorithms have been implemented for detecting vessel edges: an entropy operator (93) and a standard thresholded first derivative test. These operators are preceded by histogram equalization and edge-enhancement (LoG) operators. These edges are tracked along the vessel using the double-square-box method (94). From these detected edges, vessel centerlines and vessel diameters are determined which are then used for the reconstruction. An extensive user interface has been developed for manual correction and definition of vessel edges and landmarks which are used in verifying the accuracy of the edges and identifying vessel pairs in the two projections.

3) The 3-D reconstruction algorithm (described in detail in (2)) performs backprojection of paired vessel centerline points by a recursive traversal of the data structure, branch by branch. Corrected centerline points are backprojected from the image intensifier surface back to the x-ray source thus accounting for the system's cone-beam geometry. Second-order errors cause the backprojection lines corresponding to the same point in two different views to most likely not intersect. A practical solution is found by solving for the point in 3-D space which minimizes the distance between the projected lines. A novel aspect of our approach is that even though it uses absolute system calibration for 3-D reconstruction it also makes use of any identified landmarks to reduce these second-order errors. Landmarks are used to match corresponding pairs of projected 2D points in the two images. A corresponding point is determined by the intersection of a guideline with the center line of the arterial branch in the other view. Guide lines are computed using the geometry of the acquisition system, but if there are errors in the reported geometry the guidelines will be off (small errors reported in the rotation angles cause the guideline to appear translated in the image). To compensate for this error, landmark points are identified in each image, and an adjusted guideline is produced that is parallel to the original one but shifted by the distance between the original guideline and the corresponding landmark point. Thus, the adjusted guideline for a landmark point is forced to go through the corresponding landmark point in the other view. Guidelines for points between landmarks are adjusted by a weighted average of the adjustments for the surrounding landmark points. The weighting is determined by the distance of the point to each of the landmarks. After the 2D coordinates for the corresponding points have been found in this manner, the 3D solution is computed directly from the 2D coordinates and the reported acquisition geometry. No correction of the reported geometry is attempted based upon the landmarks. Once the vessels and landmarks are identified, the reconstruction takes less than 17 secs using a slow Sun 3/160 computer.The reconstructed solution is stored in a hierarchical data structure and is available for analysis, iterative improvement through user interaction, graphical rendering, or output. Importantly our algorithm works for any arbitrary (not necessarily orthogonal) set ($\geq$2) of orientations. Thus in addition to being useful for reconstructing simultaneous, biplane angiograms, it may be used for reconstructing several end-diastolic gated projections to improve vessel definition.

4) For visualization, a computer model of the arterial structure is generated and rendered (2). A geometric modeling software package called MAX (92), developed in part by one of our co-investigators (JP) is used to represent the reconstructed 3-D models. The data structure is designed to be easily modified to support other formats such as that of Wavefront Technologies Imaging System (95).

5) Preliminary validation of this methodology has been performed using simulations, phantoms and patient studies. Importantly, our simulation studies predicted less than a 1 mm rms error in the 3-D location of the vessel centerline for expected acquisition errors such as RAO/LAO or Caudal/cranial angular errors of up to 10 degrees and for errors in the distance between x-ray source and detector of up to 5 cm (Figures 1a, 1b and Appendix 3.2). Several copper-wire phantoms simulating a variety of left and right vascular distributions and stenosis sizes and locations were built by one of our cardiologist (LK). Reconstructed absolute vessel diameter and distances between landmarks to actual measurements taken from the phantom correlated highly with measurements taken from the actual phantom (2). RMS error of the reconstructed vessel radius varied from .26 mm for the left main coronary artery to .08 for a distal circumflex branch (2). More recently we have performed a more extensive validation in more phantoms resulting in even smaller though systematic errors (17). A preliminary clinical evaluation has also been performed (3). Two experienced angiographers were asked to score how well projections from the 3-D angiograms correlated with a similar view on the cine film in terms of vessel orientation and size (0 = no correlation to 4 = excellent correlation). In 12 views, of 30 vessels taken from 4 patient studies the score averaged 3.77 $\pm$ .46 for orientation and 3.0 $\pm$ .92 for vessel sizing (Figure 2, 3 and {1}7-10)). We recently extended this study to include 30 views from 10 patients resulting in even better results.

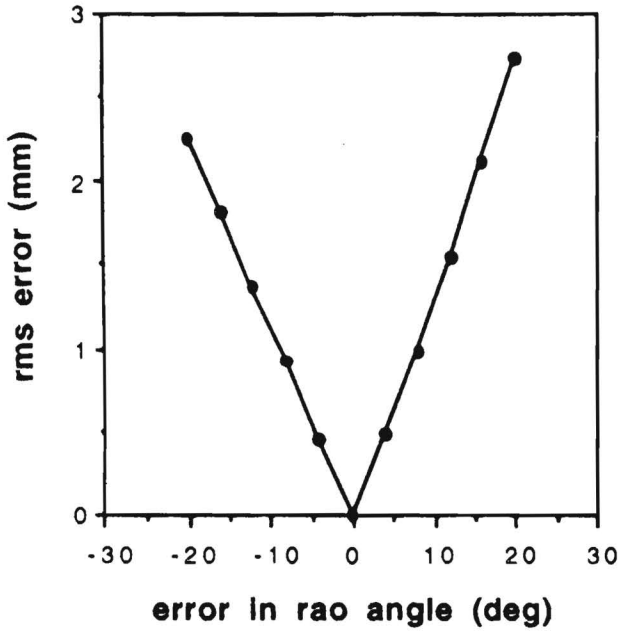

Figure 1a. RMS error in locating 3D vessel centerline when an error occurred in measuring the intensifier's RAO kappa angle.

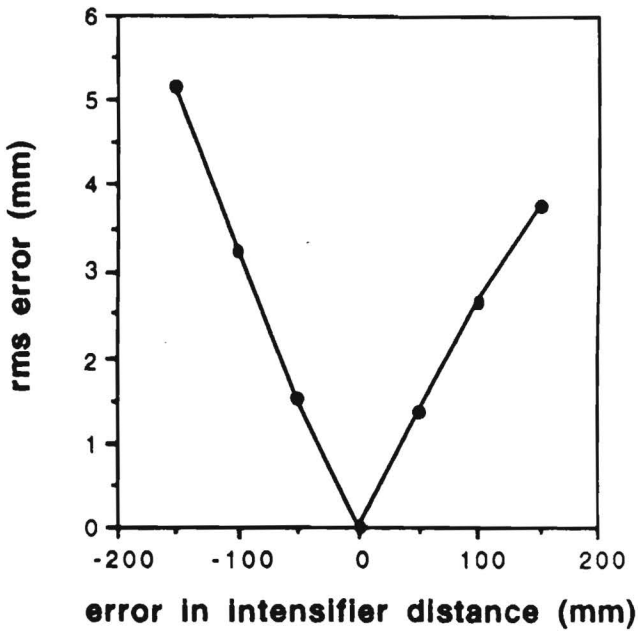

Figure 1b. RMS error in locating the 3D vessel center line when an error occured in measuring the RAO source-to-intensifier distance.

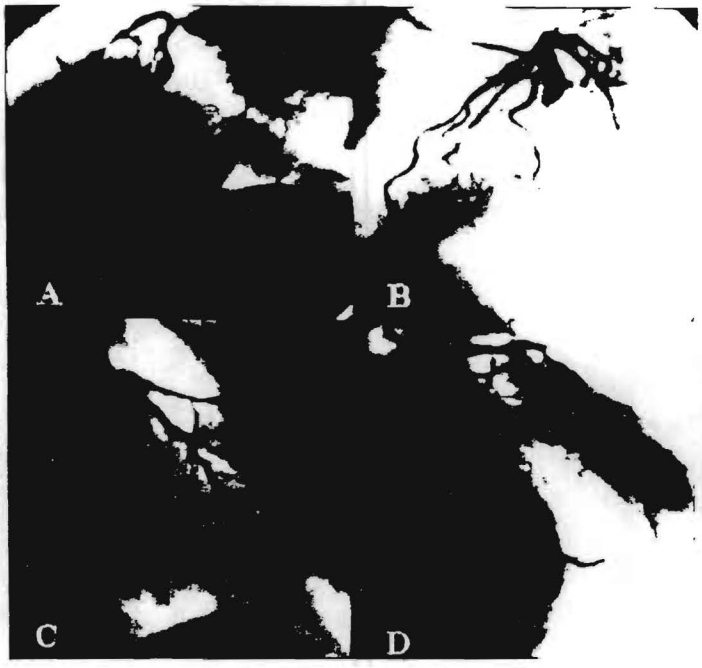

Figure 2. Left coronary angiograms in various views taken from 4 patients with diffuse atherosclerosis. A) Left anterior oblique (LAO) projection from patient 1. B) LAO with cranial angulation from patient 2. C) Right anterior oblique (RAO) view from patient 3. D) RAO with caudal angulation from patient 4.

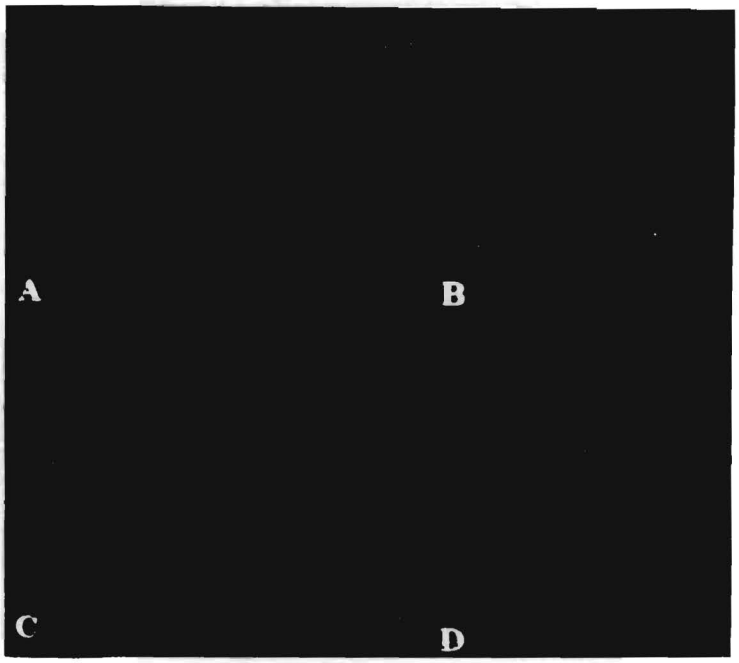

Figure 3. Corresponding shaded projections of the 3 dimensional model from the patients in figure 2. The models are reprojected into the identical angle as the actual angiographic views and displayed in the same order as figure 2. Note how well the reconstructed angiograms vessel size and orientation correspond with the actual angiogram in these difficult patients with diffuse disease. For detailed results in these patients see appendix 1, figures 7-10.

In the approach that we have taken each of the phases or modules of the reconstruction process described above are independent from each other. Thus we can use any of variety of edge detection algorithms while keeping the rest of the modules constant. Two areas which need improvement are the automatic labeling (pairing) of the branches (i.e. identify the 1st diagonal branch on each view, etc) and improve the edge detection method particularly to process an entire temporal sequence and/or to identify two vessels that cross at some point in the cardiac cycle (particularly end-diastole). We have initiated two preliminary studies to address these problems. The first one, which we intend to continue to pursue, uses active contours (4) (known as "snakes") to track the trajectory of the vessel within a frame where there is no overlap and then to use that initial result to track the vessel from frame to frame. The second study uses a model-based approach to automatically identify the vessels using multiresolution (5). The model-matching process uses explicit sensor information obtained at the time of acquisition to project the 3D models onto the multiple image planes, this being done at different levels of spatial resolution. Although this approach is promising it requires extensive development. Thus we will implement a knowledge-based approach similar to Garreau's (62) with which we have related experience (96 and Appendix 3.1).

Project 2. Extensive progress has been made towards all phases of the development and validation of methods for the quantification and visualization of 3-D myocardial perfusion and thickening distributions.

1) We developed a novel sampling method which more accurately extracts the 3D myocardial perfusion distribution using a combination of spherical coordinates for sampling the apical region and cylindrical coordinates for sampling the rest of the myocardium (6,7)(Figure 4) This novel sampling method forms the basis for a new, copyrighted software package for quantification and polar display of Tc-99m sestamibi myocardial perfusion distributions (8). This package which was developed in collaboration with Cedars-Sinai in Los Angeles is named **CEqual™** (Cedars/Emory quantification). This package has undergone successful in-house and multicenter validations (8,18,19) using close to 200 patients. CEqual™ has successfully undergone the FDA's 510(k) process for distribution in the GE and Siemens systems, and is currently being implemented on virtually every manufacturer's nuclear medicine systems.

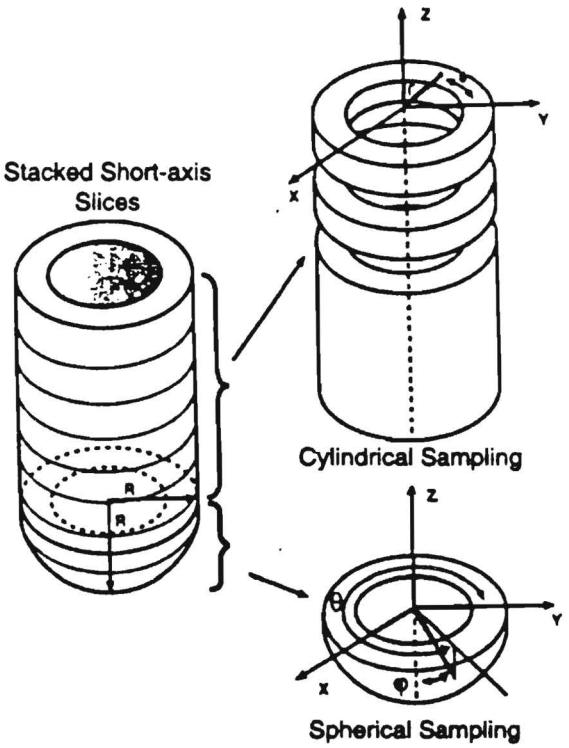

Figure 4. Maximum count circumferential profiles are automatically generated from the short-axis slices using a 2-part sampling scheme shown in this figure. First the apical cap is identified as stacked, short-axis slices that form a hemisphere; i.e. the radius of the top slice is equal to the depth of the stack. The apical cap is sampled in a spherical coordinate system as seen in the bottom right. Each point in the profile represents the maximum counts per pixel encountered along the radius of search for each phi and theta angular sample. The remaining portion of the myocardium is relatively cylindrical in shape and is sampled slice by slice using a cylindrical coordinate system (top right). The 3D coordinates of each myocardial maximal count sample are stored for subsequent 3D rendering.

2) Algorithms were developed which utilize the 3D coordinates and corresponding counts of the samples extracted using the above method for quantification and visualization of the 3D myocardial perfusion distribution using the actual dimensions of the left ventricle (6,7)(Figure 5 and {1}11-13). In a study of 26 patients who underwent rest/stress sestamibi imaging we showed that the new sampling method and 3D display was equal or superior to polar map approaches (and even to slice-by-slice interpretation) in assessing defect size, location and severity (9,22). In another study of 24 patients with left bundle branch block

(LBBB) who underwent Tl-201 stress/delay imaging we showed that the 3D myocardial perfusion display approach helps differentiate LBBB patients with CAD exhibiting a large heart and apical hypoperfusion from patients with LBBB and no CAD (10). Siemens and ADAC have contracted with us to implement this copyrighted 3-D software package (called PerfSPECTive™) on their systems.

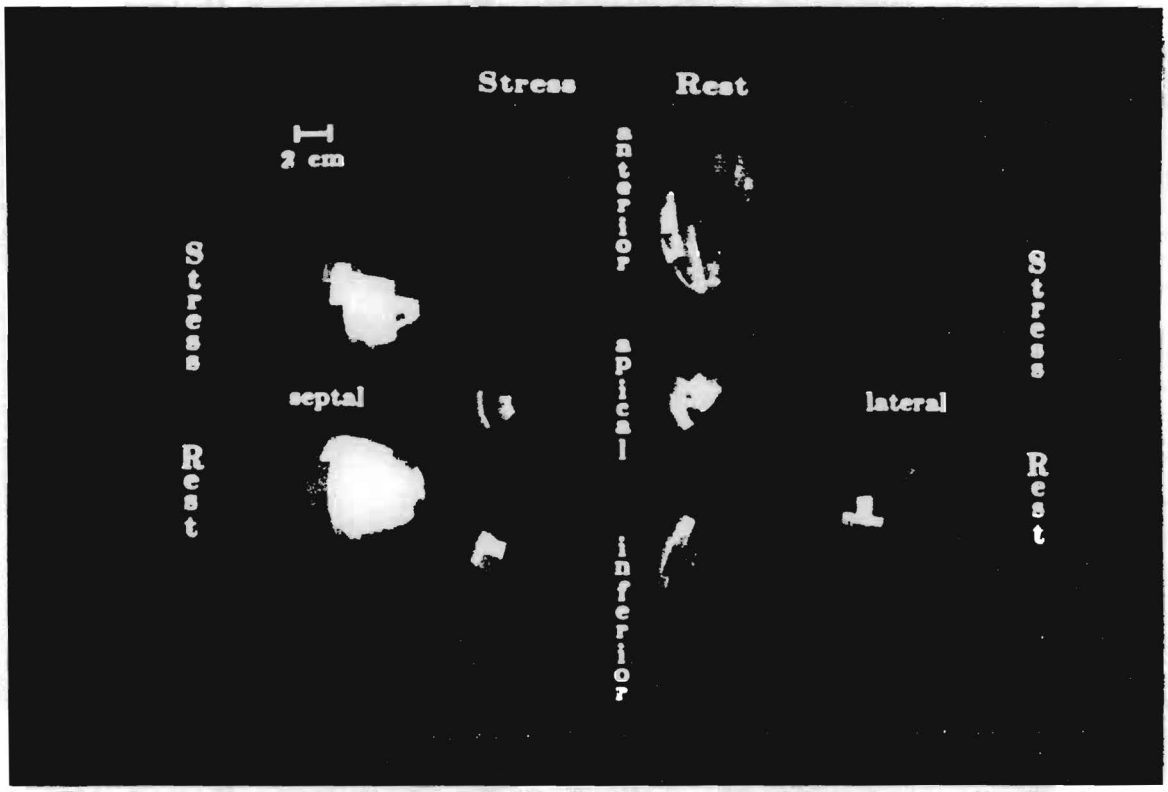

Figure 5. This is a panoramic display of 3D Tc-99m sestamibi perfusion distributions at rest and immediately post-stress. The perfusion is displayed with multiple 3D models depicting the shape of the left-ventricular myocardium and displayed in 5 views to allow visualization of all regions of myocardial perfusion. The two models on the left show the septal aspect of the myocardium, with the stress on top and the rest below. The two models on the right show the lateral aspect of the myocardium with the stress on top and the rest below. The six models in the middle of the figure (displayed vertically), demonstrate the anterior aspect of the myocardium at the top, apical aspect in the middle, and inferior aspect at the bottom, with stress on the left and rest on the right, respectively. A scaling factor of 2cm is seen in the upper left of the figure. In this particular case, stress perfusion abnormalities are noted in the antero-lateral and apical region which is nearly normal at rest. There is also noted a large inferior perfusion abnormality which is unchanged between stress and rest.

3) A novel algorithm was also developed to quantify and visualize Tl-201 myocardial perfusion defect reversibility between stress and delay as a marker of myocardial ischemia (11). The method was prospectively validated in a multicenter trial using 140 prospective patients (12). This copyrighted algorithm was incorporated into the well-known Emory's Bullseye program and is currently used all over the world. The same algorithm has been validated in a multicenter trial on 101 patients undergoing rest/stress Tc-99m sestamibi studies and incorporated into the CEqual™ program (19) and in our 3D visualization scheme.

4) Directed in part by the June 1988 Study Section concern that determining myocardial mass from SPECT might be difficult due to poor resolution and in some patients absence of flow (and thus counts), we replaced this approach with a count-based determination of systolic wall thickening. We agree that with the relatively poor resolution of cardiac SPECT studies it is impossible to accurately measure the wall thickness of the LV using geometric methods (85). However, we have shown, both theoretically and experimentally, that myocardial wall thickness is linearly proportional to the maximal counts extracted from the myocardium (13), making the measurement of LV wall thickening a possibility using a multiple gated SPECT acquisition and Tc-99m sestamibi. Recently we have used our 3D sampling scheme and Fourier analysis (phase analysis) of 8 temporal samples per myocardial segment to quantify % systolic wall thickening (SWT) as twice the amplitude of the 1st harmonic =(end-systole(ES) - end-diastole(ED)) divided by ED times 100 (14). The method was tested in 28 patients and showed that this quantification agreed favorably with the visual assessment of SWT

and importantly that it had a high predictive value for viability as assessed by comparison to resting sestamibi distributions (15). More recently we have also quantified the phase of the wave of onset of thickening and have developed normal limits for both SWT and phase (16). We have shown that even in regions with very low counts which are dyskinetic the phase is properly determined to be about 180 degrees out of phase with the rest of the ventricle (Figure {1}14-16). We are continuing our development of 4D (3D + time) animated display of these distributions.

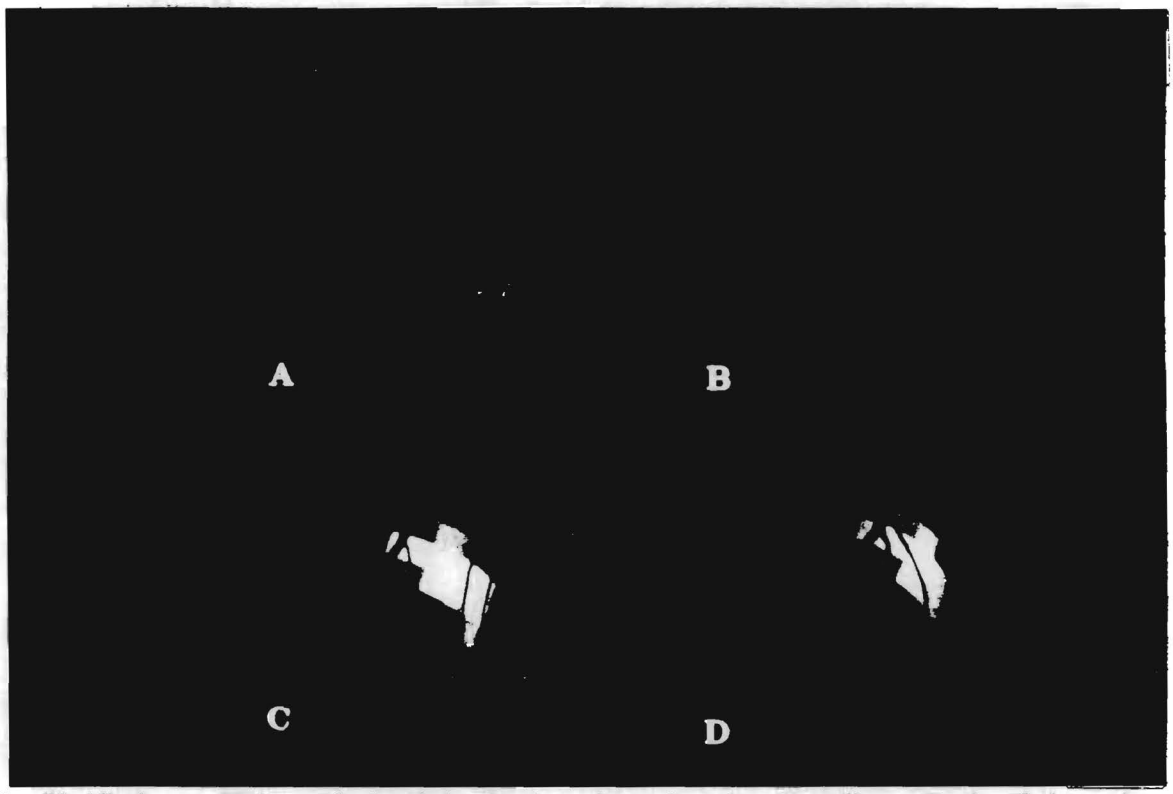

Figure 6. Unified anatomic and physiologic data from 3 animal studies. Each of these images is the superimposition of the reconstructed 3D coronary angiogram onto the Tc-99m Sestamibi perfusion data. The normal coronary arteries are shaded red with a transition to green at the site, and distal, to the balloon occlusion. The coronary angiograms were performed both before and after balloon occlusion to allow reconstruction of the normal vessel (red + green), and the site of the balloon occlusion (red/green interface). The perfusion data is plotted on the surface of a shape depicting the left ventricular myocardium. Lighter colors indicate more perfusion with darker colors indicating relatively less perfusion. Images 6A) and 6B) are data taken from pig #252. Image 6A) is a view from the septum. The vessel on the right is the left anterior descending (LAD) and courses in the anterior interventricular groove. The vessel on the left is the distal half of the right coronary artery (RCA) with the 2 larger branches identifying the posterior descending artery and left ventricular branch. The more proximal RCA is not shown as it courses relatively far from the left ventricle in the atrial - ventricular groove. Image 6B) is the same data as 6A) but viewed from the anterior perspective. The LAD is seen on the top coursing to the apex. The circumflex (LCX) courses laterally to the right near the base. Obtuse marginal, and diagonal branches are seen to course laterally from the LCX and LAD. In both A) and B) the purplish colors seen at the apex and apical-septum of the perfusion model indicate the decreased perfusion caused by the very short balloon inflation in the mid segment of the LAD (identified where the vessel turns green). From this angle the RCA is not in the view. The darker colors seen in the basal perfusion display correspond to the membranous septum. Image 6C) is data from pig #338. The view is the same as 6B). In this case a longer duration of balloon occlusion in the mid LAD resulted in a more severe perfusion abnormality at the apex seen as green and black on the perfusion map. Image 6D) is data from pig #502 seen from the anterior projection. The balloon placement in this study was more distal in the LAD resulting in a decrease in apical perfusion. Note how well the sites of coronary occlusion and the perfusion defects correspond. Additional figures relating to the animal projects are contained in Appendix 1, (figures 17-30).

Project 3. Progress has been made towards the unification of the coronary tree superimposed on the myocardial perfusion distribution.

1) Initially the vascular tree was manually registered such that the proximal segment of the left anterior descending tree was aligned with the anterior interventricular groove as identified on tomographic slices of myocardial perfusion. This approach was tested by independently imaging the copper-wire models superimposed on a LV myocardial perfusion phantom. These phantoms were positioned such that a simulated stenosis was located in the center of the simulated stress perfusion defect. This manual registration yielded reasonable agreement between the experimental and observed configurations (2), but the process is cumbersome, subjective and somewhat imprecise. Recently we have developed and implemented an automated method in which the operator "picks" three points in the 3D model of the coronaries and one point on the interventricular groove. The computer then automatically performs all the appropriate translations and rotations to align the two distributions and then, if desired, slightly warps the vessels to fall above the myocardium (Figure 6 and {1}17-31). This proposal aims to further improve this unification by using the shape from the ED sestamibi tomograms (rather than the averaged non-gated slices) and by improving our 3D filtering of the shape of the 3D perfusion distribution.

2) In response to concerns from the June 1988 Study Section, considerable effort has been spent in developing the appropriate animal model to validate the unification algorithm which is described in detail in the Methods section. We switched from a canine model to a swine model. This was done for two reasons. The first few dog experiments performed illustrated that the size and length of the dogs coronaries are significantly smaller than humans thus not providing an appropriate standard. Pigs vessels are significantly larger and their distributions much more like humans. Second, the pig model was also chosen in consideration of the Study Sections concerns about the influence of collaterals or our results. It is well-known that pigs rarely have any collaterals whereas dogs' collaterals are usually abundant. A myocardial region supplied by collaterals will show normal perfusion even though the major vessel supplying it might be occluded thus invalidating our experiment. The difficulty with pigs, as an experimental model, is that since their hearts are not supplied with collaterals even small infarcts can cause the animal to arrest. Thus we switched from inducing ischemia or infarction to simply relating the 3D location of an inflated balloon to the perfusion distribution created by an intracoronary injection of sestamibi proximal to the inflated balloon. We have successfully performed these experiments in the last five consecutive pigs imaged.

3) To test the clinical utility of the technique 16 patients have been acquired and processed who have undergone both biplane angiography and Tl-201 myocardial SPECT imaging. Unification was delayed pending validation of the automated methodology.

4) Publications (Published or in press)

1. Peifer JW, Mullick R, Ezquerra NF, Hyche E, Garcia EV, Klein L, Cooke CD: Coronary Vasculature Visualization from Limited Angiographic Views. Proceedings of the First Conference on Visualization in Biomedical Computing, Atlanta, GA, May 22-25, IEEE Catalog # 90TH0311-1, pp 195-200, 1990.
2. Peifer J, Cooke D, Klein L, Garcia EV: Quantification and Visualization of 3D Cardiac Imagery. IEEE Trans on Biomed Eng, Vol. 37, No. 8, August 1990.
3. Klein JL, Peifer JW, Ghazzal MB, Ezquerra NF, Cooke CD, Garcia EV: Three Dimensional Representation of Patient Coronary Arteries: A Preliminary Clinical Evaluation. Circulation, Vol. 84, 4:II-721, 1991.
4. Hyche ME, Ezquerra NF, Lawton D: Vasculature Detection Using Active Contours. Proceedings of the International Conference of the IEEE EMBS, Nov. 1991, Orlando FLA. (abstract in Press)
5. Hyche ME, Ezquerra NF, Lawton D: Model-Based Identification of Vasculature from Angiograms Using Multiresolution. IEEE Computers in Cardiology Abstract book. Conference in Venice, Italy, Nov 1991. (Published but not presented in Italy due to lack of travel funds)
6. Cooke CD, Garcia EV, Folks RD, Peifer JW, Ezquerra NF: Visualization of Cardiovascular Nuclear Medicine Tomographic Perfusion Studies. Proceedings of the First Conference on Visualization in Biomedical Computing, Atlanta, GA, May 22-25, IEEE Catalog # 90TH0311-1, pp 185-189, 1990.
7. Garcia EV, Cooke CD, Van Train K, Folks RD, Peifer JW, DePuey EG, Maddahi J, Alazraki N, Galt JR, Ezquerra NF, Ziffer J, Berman D: Technical Aspects of Myocardial SPECT Imaging with Tc-99m Sestamibi. Am J Cardiol, 1990;66:23E-31E.
8. Van Train K, Areeda J, Garcia E: Development and prospective validation of quantitative same-day Tc-99m sestamibi SPECT. Circulation 84(4) II-304, 1991. (abstract)
9. Cooke CD, Ziffer JA, Folks RD, Alazraki NP, DePuey EG, Van Train K, Maddahi J, Berman DS, Garcia EV: Optimal Methods for Sampling and Displaying Tc-99m Sestamibi Myocardial Perfusion Studies. J Nucl Med, 32(5), 1006, 1991. (abstract)

10. Ziffer JA, Cooke CD, Krawczynska EG, Garcia EV*: SPECT Thallium-201 in Patients with Left Bundle Branch Block: Utility in Assessing Apical Perfusion and Ventricular Size in 3-Dimensions. J Nucl Med, 32(5):1034, 1991. (abstract)
11. Klein JL, Garcia EV, DePuey EG, Campbell J, Taylor AT, Pettigrew RI, D'Amato P, Folks R, Alazraki N: Reversibility Bullseye: A New Polar Bullseye Map to Quantify Reversiblity of Stress Induced SPECT Tl-201 Myocardial Perfusion Defects. J Nucl Med, 31:1240-1246, 1990
12. Garcia E, DePuey EG, Sonnemaker RE, Neely HR, DePasquale EE, Robbins WL, Moore WH, Heo J, Iskandrian AS, Campbell J:Quantification of the Reversibility of Stress Induced SPECT Thallium-201 Myocardial Perfusion Defects: A multicenter trial using Bull's-eye polar maps and standard normal limits. J Nucl Med 1990; 31:1761-1765.
13. Galt JR, Garcia EV, Robbins W: Effects of Myocardial Wall Thickness on SPECT Quantification. IEEE Trans Med Imaging 1990, 9(2):144-150.
14. Cooke CD, Ziffer JA, Folks RD, Garcia EV: A Count-Based Method for Quantifying Myocardial Thickening from SPECT Tc-99m Sestamibi Studies: Description of the Method. J Nucl Med, 32(5):1068, 1991. (abstract)
15. Ziffer JA, Cooke CD, Folks RD, La Pidus AS, Alazraki NP, Garcia EV: Quantitative Myocardial Thickening Assessed with Sestamibi: Clinical Evaluation of a Count-Based Method. J Nucl Med, 32(5),1006, 1991. (abstract)
16. Cooke CD, Garcia EV, Folks R et al.: Myocardial thickening and phase analysis from Tc-99m sestamibi multiple gated SPECT: Development of normal limits. Abstract accepted to SNM '92.

2.D EXPERIMENTAL DESIGN AND METHODS

The experimental design and methods for this renewal application will be discussed in terms of six proposed tasks, Projects 1 through 5. A schedule for the four-year research program in terms of these five projects is given in Figure {1}-0.

The algorithms and techniques will be developed (or translated) in the context of UNIX, X-windows based environments to ensure the optimal framework in terms of standardization, portability, compatibility, and ease-of-use of the software resulting from this research. Some special-purpose software will be utilized in the research (i.e., NeuronData's Nexpert Object and either Wavefront Technology's Advanced Visualizer or Digital Equipment Corporation's Application Visualization System) to facilitate and expedite the research while at the same time conform with emerging standards in software engineering (e.g., C-language code, the GL graphics library of primitives, and imbeddable/callable routines supporting UNIX and X-windows).

PROJECT 1. QUANTIFICATION AND VISUALIZATION OF ANATOMIC INFORMATION

1.1 Sensitivity Study. This project is to establish the sensitivity of an acquisition error on the reconstructed vascular model. In this project we will continue to develop a simulation system which uses the arterial reconstruction program on either simulated or real vascular trees to study the propagation of acquisition errors on the accuracy of the three dimensional reconstruction of vessel centerline and cross-sectional area. In Section C we showed how this simulation predicted less than a 1 mm rms error in the 3-D location of the vessel centerline for expected acquisition errors. We will extend this analysis to include 30 vascular models (10 phantoms, 10 animals and 10 patients, 20 left & 10 right coronary vasculatures) to assess the propagation of the rms error of location and cross-sectional area due to errors in the following parameters: a) angular errors (RAO, LAO, caudal and cranial), b) distance errors (x-ray source to image intensifier for each view), c) movement between views (even in simultaneous biplane systems there is at least a 1/15 to 1/30 sec delay between views). The methodology consists of the following steps: accepting a reconstructed model as the gold standard, introducing a known error in the acquisition parameter, reconstructing a new model with this error, comparing model with error to model without, record the reconstruction error, increment the magnitude of the acquisition error, repeat. To assess the potential of single-plane ECG gated reconstructions and of reconstructions with more than two simultaneous views (and the rest ECG gated) the simulation will compare the reconstruction from two simultaneous views to one with views from different beats. The methodology will be tested for N-views. See Appendix 3.2.

1.2 Automation of vessel reconstruction. As reported in Section C, the methods presently used to detect features, track vessel segments, and construct corresponding feature sets between two views simultaneously will be incorporated into the proposed approach. The thrust of the approach is two-fold: to further automate the vascular detection and reconstruction processes, and to more fully integrate the temporal dynamics of the moving heart in the quantification process. There are three distinct and novel characteristics of the overall approach: firstly, the approach is in itself "unified" as it relies on information derived spatially (from different views) and temporally to help resolve situations associated with missing data and/or

ambiguous structures; secondly, an object-oriented environment will be utilized ;thirdly, extensive use of a priori knowledge (both geometrical and anatomical) will be used to build a knowledge base.

The approach consists of a three-tier image understanding architecture: a low-level vision tier for feature extraction; a middle tier associated with perceptual grouping, where initial label assignations will be made to vessel structures using the extracted features via a knowledge base; and a high-level vision tier, which uses meta-level rules for overall process control and to resolve ambiguities and guide the labeling processes by intelligently using spatial-temporal information and anatomical knowledge (see Appendix 3.3-3.5).

The quantification process begins by introducing corrections to account for image distortions and magnification as described (2).

The control module then initiates the quantification procedure by selecting a seed or starting point. The seed will be defined as the vascular tree root, where the assumption is made that the tree root has the highest grey level contrast. The root will be found as follows. A time-integrated image will first be constructed which is simply the addition of all of the frames for the sequence to be analyzed; this sum image gives a gross estimation of the spread (over time) of the high-intensity areas in the image. The intensity values of the sum image will be projected onto the vertical and horizontal image axes, giving rise to two intensity histograms, such that the regions containing the high-intensity local regions will show as local maxima in these orthogonal histograms. Adding the heuristic that the root is likely to be found in the upper half of the image (better localized depending on acquired view), an initial region of interest will be defined in which to search for the edges of the tree root in the first frame of the sequence.

The control (high-level) module activates the tracking procedure, consisting of a modified double-box tracking method (56, 23).

As (non-ambiguous) image features are detected, a database is updated containing the coordinate information in the chronologically ordered sequence of detection. Once again, the database is hierarchical and object-oriented in nature, such that, as the features are identified (with their corresponding certainty values), this feature information is stored as labelled objects with anatomically meaningful labels. The tracking procedure proceeds until the first region of ambiguity (ROA) occurs. The information associated with the ROA at that point is passed to the second or middle tier which performs perceptual grouping operations. Since the information is retained both numerically (i.e., in terms of widths, coordinates, lengths) as well as symbolically (through labelled objects), the resolution of the ambiguity will be first explored at this level by applying a priori knowledge in terms of rules.

A similar analysis is independently conducted in the second view. At the ROA point, again the information from the tracking procedure is introduced to the middle-tier knowledge base. At this point, the ROA has been considered in both views independently, and the conclusions reached by both resolutions are then passed on to the third (control) high-level image-understanding tier. At this level, the meta-level rules consider the inferred resolutions of the ROA in each view. If there is agreement, this control tier gives the go-ahead to continue tracking along each of the two new vessels found in the two views. If there is a conflict between the two proposed resolutions, or if the two proposed resolutions do not support the same conclusion equally strong, the control module activates the temporal sequence. At this point, the first box containing tree root in the first frame is mapped onto the next frame in the sequence, and the process of tracking is initiated in the second frame; the same procedure is followed in the second view, second frame. With the activation of the temporal sequence, an additional detection independent scheme is also activated, based on active contours [5,24], as explained in the Progress Report Section. This active contour, or snake, will be placed at the location of the centerline in the previous frame, and directed through the energy functional to move in a particular direction, based on a priori knowledge of the point in the cardiac cycle.

The control module will construct a bookkeeping record of the ROA that is undergoing resolution, until the same hypotheses are reached in both space and time with corresponding certainties that agree within a predetermined range (to be determined experimentally). The activation of the analysis of a subsequent frame in the temporal sequence performs the procedure using the low-level operators and the active contours within the tracking box. If the conflict is not resolved, or is taking too much time, the operator will either be invited to intercede or will be allowed to interrupt the procedure.

In terms of process termination, there will be a multi-step process followed. Initially, the process will be terminated "high" in the tree. For instance, for the left artery, the process will terminate after labeling and characterization of the left main, LAD, LCX, diagonal, septal, and obtuse marginal arteries. The process will terminate automatically if conflicts are unresolved, or terminated by the operator. As the methodology undergoes testing and verification, additional branches will be attempted. In addition to this approach, an attempt will also be made to allow the operator to define a termination point interactively, and the process of quantification or labeling will proceed until the predetermined termination point is reached. Once the desired portion of the tree has been quantified, confirmed by the degree of certainty of correct labeling, and approved

by the operator, the reconstruction process is initiated. In this regard, the 3D reconstruction becomes straightforward, as the labeled information is at that point properly labelled and retained in the hierarchical database.

This model representation will be explicitly stated in terms of symbolic rules, as in the foregoing examples. The certainty factors and the validity of the rules themselves will be rigorously tested experimentally in project 5.2, as systematically done in the construction of rule-based systems. However, this framework has been shown to work well in the case of coronary tree reconstruction and labeling (62), and in our experience in the case of interpretation of cardiac imagery using the Certainty Factor Model (96,97 and Appendix 3.1). These preliminary results, coupled with the results obtained using active contours and morphological operators, have amply demonstrated the reliability, accuracy, and robustness of the approach.

1.3 Manual editing. This project is to continue to develop the user/computer interface so an operator (quickly) manually performs all of the automated tasks described above. This will ensure that difficult or complicated studies can still be analyzed. In addition the automation software described above will be designed such that, at numerous stages of decision-making, the user/operator will have the option to undo what the program has done, and intervene manually to correct errors. Although this program has undergone extensive development (over 5,000 lines of code), improvements are frequently suggested and rapidly implemented.

1.4 Temporal Visualization. There will be a 3D arterial tree for each temporal pairwise reconstruction. For visualization purposes, the most direct fashion of dynamically displaying this information will be to initially use a cine-loop sequence that cycles through the frames along the cardiac cycle. To enhance this visualization, the entire tree can be rotated, such that the resulting visualization resembles a "beating" tree that goes around. Once this is accomplished, a more dynamically interactive method will be employed, wherein the user can change the viewing perspective in real time, and such that the user can stop or start the "beating" motion at different perspectives.

1.5 Stenosis characterization. Now that we have significantly improved our vessel definition and reconstruction program we will retry to implemented ellipsoidal vessel cross-sections (rather than circular) which previously appeared as twisted vessels. We will also investigate mapping the "texture" (intensity modulation) of the angiographic projections onto the 3-D vessel for improved characterization of the stenosis.

PROJECT 2. QUANTIFICATION AND VISUALIZATION OF PHYSIOLOGIC INFORMATION: PERFUSION. The main objective of this project is to further develop a 3D representation of myocardial perfusion which will be extended to include temporal changes throughout the cardiac cycle. The main model which will be further developed to represent these 3D distributions is a patient-specific (actual) heart model.

Method of Procedure: Myocardial perfusion tomographic scans will be performed using mainly 8 frame multigated Tc-99m-sestamibi SPECT or in some clinical projects non-gated Tl-201 SPECT. Tl-201 acquisition and processing will be performed as per (78), but will include reinjection at rest. Sestamibi SPECT studies will be performed following our optimized one-day rest/stress methodology (8). Commercial software will be used to gate the projections and for reconstructing and displaying in cine format each of the moving slices. The gated projections will be combined to form three sets of data: 1) a 8 frame multigated set, 2) a single frame per projection obtained from the sum of the 8 frames, and 3) an "end-diastolic" projection where 3 of the 8 frames are retained and summed to eliminate the blur due to wall motion.

Analysis of perfusion distributions will consist of extracting maximal count samples using our new 3-D sampling scheme as described in the Progress Report. These profiles are compared to normal limit profiles to identify hypoperfused and reversible regions in patients (13,14,18,19,75,78 etc) and in animals (98,99). These 3D maximal count arrays are converted to our newly-developed polar maps (Bullseye displays) using the approach in (8) in order to represent the 3D information in 2D. These 2D polar maps will continue to be compared to the 3D methodology of this proposal.

2.1 Improved shape representation of actual heart model. As described in (7) the current shape of 3-D model of the myocardium constrains each slice to be circular by applying a least squares fit to the 3-D cartesian coordinates (triplets) extracted using our sampling scheme. Although this was beneficial for low-count, non-gated smeared Tl-201 studies it is a limitation for the gated, higher count Tc-99m sestamibi studies since it distorts the true shape of the myocardium. This subproject is aimed at improving the myocardial shape by implementing the following methodology. The triplets are already converted to cylindrical coordinates (radius, theta, length) for the basal side of the sampling and to spherical coordinates (radius, theta, phi) for the apical side [Figure 4]. A two dimensional "image" will be constructed from these coordinates by having the x-axis represent theta (0-360 degrees) and the y axis represent length (from the base=0 to the maximum length) and phi (from the interface of the basal to apical region to the apex). The magnitude of the radius will be assigned (to modulate) to each pixel. This 2D "image" is then filtered using

our standard filtering programs. Before filtering a 2D operator will replace the value of a specific radius by that of the weighted average of its neighbors if the value of the radius is greater than a threshold to be determined. Once the image is thresholded it will be filtered. Hann and Butterworth filters will be investigated first. Once filtered a new 3-D model will be rendered using the coordinates generated by this image. The same process will be performed in 4-dimensions for temporal studies (i.e. use a 3D filter on a 4D data set). Since these are radii of maximal counts samples they represent the middle of the myocardium between epicardium and endocardium. A constant .5 cm will be added to these radii when epicardial models are needed to unify with the vasculature. We will also investigate interpolation of the radius image and the corresponding 3-D count array in order to reduce the size of the samples being displayed.

The shapes generated from this procedure will be compared to shapes obtained from gated MRI studies (see project 3.1). After 3-D registration of the two studies a similar shape "image" will be extracted from the MRI study and the two images will be compared. The thresholds and filters which minimize the rms radius will be selected as optimal.

2.2 Quantification of myocardial perfusion defect size (extent) and severity. All measurements will be performed for the three sets of data (when available) described above: multigated, combined single frame and end-diastolic frame. The dimensions of the LV myocardium to be measured are the radial distance from the long axis reference line. As above, for each of the 3-D myocardial samples, the filtered radial distance from the long axis reference line to the maximal count voxel representing the center of the myocardial wall will be calculated and stored in a 3-D array per frame. These arrays will then be passed on to the graphics editor for 3D representation.

In order to quantify the extent of hypoperfused myocardium, perfusion defects are identified as pixels with normalized maximal counts falling below the corresponding lower limits of normal profiles similar to the methodology in Appendices 2.11,2.12,3.1,3.6. In addition, the number of standard deviations (SDs) below the mean normal profile, for each of the points in the 3-D arrays, will be determined and stored for a measure of defect severity. Identification, in patients undergoing Tc-99m sestamibi or Tl-201 studies, of stress perfusion defects as being ischemic or necrotic will be performed using the quantitative reversibility methodology described by in the progress report (11,12,19). The quantitative extent of ischemia will be the main parameter compared between these methods. Quantification of the total myocardial mass (TMM) and perfusion defect extent (PDE) will be performed using an equation similar to one previously used by the PI (98,99).

TMM = Sum over all i pixels $[(2\pi/40) \times Ri \times Ti \times Sl \times cf]$ [Eq. 2.1] where for each ith pixel, Ri = radius from radius image, Ti = thickness from thickness array (border definition using MRI when available), Sl = slice thickness (6.25mm for SPECT) and cf is the conversion factor of myocardial mass per voxel = .25 grams (.625cm cubed times specific gravity of myocardium 1.05 gms/cc). PDE will be quantified using Equation 2.1 but summed only over all abnormal pixels. The percent hypoperfused myocardium determined from above (% hypo = 100 x PDE/TMM) will be compared to the methodology described in (98,99) where the % of the maximum count profiles falling below normal are multiplied by a coefficient which reflects the contribution of that slice to the total left ventricular mass (obtained from predetermined curves). Either of these two techniques will be used to identify the extent of ischemic or scarred myocardium by using pixels appropriately identified as such from the above described method (11).

Perfusion defect severity will be calculated by inserting a severity factor Si inside the bracketed term in equation 2.1, ranging from Si = 0 for normal myocardium to Si = 1 for walls with counts as low as the local background. These factors will be determined and stored for each of the pixels from the 3-D array. TMM and PDE will be validated in Project 5 using the animal model. A similar parameter to PDE will be used for determining the ischemia defect extent (IDE) for the reversible region from SPECT studies.

2.3 Visualization of Myocardial Perfusion. We will continue to use Georgia Tech's MAX graphic editor to construct a three dimensional model of the myocardium until we switch to a newer graphic editor which uses standard window environments like Wavefront, AVS and Hoops. Motion will be simulated by displaying 16, 512 x 512 projections from equally spaced angle steps 360° in an animated sequence (at practically any frame rate) on our computers (PIXAR, Silicon Graphics or SUN IPX). The axis of rotation as well as rate of display is operator selectable (in real time on the Silicon graphics preselected on the others). The myocardial models are constructed of tiles color-coded to counts, thickening, phase of contraction, MR parameters. The tiles are also coded to functional results such as to highlight hypoperfused, ischemic or infarcted points. One tile is used for each of the elements of the 3-D array making up the myocardium. In addition, the color-coded surfaces are shaded according to a predefined illumination orientation and the particular projection being viewed. Animated 3D construction and displays will be performed for the actual heart model where a single surface is used to represent the myocardium color coded for the stress/delayed/rest perfusion distribution and offering functional images where abnormally perfused tiles are blacked out

(blackout map) or color-coded to the number of SDs below the mean normal profiles (or severity factor) (See {1}-12-13). The location of the surface simulates that of the "epicardial surface".

2.4 Development of temporal visualization methodology. Using the 8 filtered 3-D arrays from the multigated SPECT studies, constructions will be performed using MAX representing the 3D heart model over 8 temporal samples throughout the cardiac cycle. The animated display will consist of 8 frames per projection x 16 projections x 256x256 matrix which is the maximum amount of display memory which may be downloaded to the PIXAR. The display will consist of the LV myocardium changing in time throughout the cardiac cycle in one projection and then rotating to the next projection where it will then again appear to contract. This display will be repeated for all 16 projections and then the procedure will be repeated indefinitely until the operator requests termination. The PIXAR will allow that this display simulate real-time contraction.

2.5 Development of method for automated groove detection. Using our approach (100) for quantifying right ventricular (RV) myocardial perfusion with Tc-99m sestamibi we will extract maximal counts distributions for the RV similar to the method described for the LV (8). The RV's main axis will be parallel to the LV's. Using the count distributions starting at the base of the heart we will automatically identify the voxels with the same 3D cartesian coordinates for the right and left as being part of the anterior and inferior interventricular grooves. Figure {1}-31 illustrates how well these grooves are visualized in 16 consecutive Tc-99m sestamibi patient studies.

PROJECT 3. QUANTIFICATION AND VISUALIZATION OF PHYSIOLOGIC INFORMATION: MYOCARDIAL THICKENING. The main objective of this project is to develop and validate a count-based method to quantify myocardial thickening as a 3-D model which will be extended to include relative temporal wall thickening changes throughout the cardiac cycle. As described in the progress section the method uses our validated hypothesis that the change in maximal counts in a myocardial sample throughout the cardiac cycle is directly proportional to the change in thickness. Method of Procedure: The methods for multiple gated acquisition, processing and sampling described for SPECT in Project 2 will be used. Additional details are as follows: The 8th array is corrected for normal end-diastolic count dropouts by setting the total counts in array 8 equal to the total counts in array 1. Each of the arrays 2-8 are then interpolated to contain the same number of samples as array 1, and all 8 arrays are subsequently spatially smoothed using a standard low-pass filter, and temporally smoothed using a low-pass filter with wrapping.

3.1 Quantification of myocardial thickening.

Emission tomography: An 8-point,one-dimensional fast-fourier transform (FFT) is calculated for each spatial sample in the 3-D arrays. Twice the amplitude of the 1st harmonic of the resulting FFT is used as an approximation of systolic-wall thickening (SWT), as shown in Figure {3.7}-2. To display the thickening information, 2 new maps are being generated:a) a relative thickening map in which each point is equal to (ES - ED) / (max of (ES - ED) array) x 100, and b) a percent thickening map in which each point is equal to (ES - ED) / ED x 100%; this map is then clipped to the range of 0 - 1000, allowing assessment of percent thickening using the colormap, i.e. colors at the top of the color scale would represent a %SWT of approximately 100% (or may be set >100%), colors near the middle of the color scale would represent a %SWT of approximately 50%.The onset of thickening (phase) can also be approximated by extracting the phase shift (in degrees) of the 1st harmonic of the FFT. A phase histogram can then be generated from the resulting phase array. To display the phase information a new map is being generated in which each point is equal to the phase shift (in degrees) of the 1st harmonic of the FFT; this map is then clipped to the range of 0 - 360 degrees for display. Preliminary normal limits have been generated for the % thickening and phase parameters (16). Limitations: One limitation of the approach is that only 8 frames are used to define the cardiac cycle. This could lead to aliasing of the temporal information resulting in an artifactually low % thickening measurement. The FFT approach significantly reduces this undersampling limitation by fitting the 8 samples to a function with infinite samples. Further improvements will also be pursued by using multiple harmonics (101). Another limitation is that since this is a count-based method inaccurate thickening will be determined if there is an abnormality which significantly reduces the number of counts. Our implementation of the phase significantly helps with this limitation as shown in Figure {1}-15-16. Note that one of the main clinical utilities of the method is to image patients injected at stress with sestamibi but imaged at rest 30 mins later. This strategy provides a simultaneous assessment of stress perfusion and resting thickening (viability) hopefully obviating the need for a second resting scan. Thus the objective is to determine whether the myocardium thickens or not rather than to measure the exact amount of thickening. Validation: We will extend our previous study to 40 patients to demonstrate whether a wall which quantitatively thickens at a hypoperfused region is predictive of a quantitatively reversible region using the resting perfusion information. The accuracy in determining the presence or absence of thickening will be established by comparison to cine MRI. If the first 10 patients

compared to MRI result in reduced thickening for SPECT, we will then switch to either 16 frames over the cardiac cycle or 8 frames from ED to ES only.

Magnetic Resonance Imaging. ECG multiple gated MRI studies will be acquired in the exact short axis orientation (dual angle of obliquity) with identical interslice thickness (6.25mm), and in the vertical and horizontal long-axis orientations. Imaging will be performed using conventional fast gradient echo cine techniques (102). Each slice will be imaged at end-diastole (at the R-wave) and at sequential 25ms intervals throughout the cardiac cycle. Endocardial and epicardial borders will be manually drawn from the short axis except at the apex where the apical region will be defined using vertical and horizontal long axis and interpolated in 3-D to the short axis corresponding to the apex. The anterior and inferior interventricular grooves as well as the atrioventricular grooves will be manually identified. Trinary slices will be generated having the value of 2 for the pixels defining the epicardial border, 1 for the endocardial border and 0 for all other pixels. This 3-D distribution will be rotated around the long axis until the grooves match those of the emission studies. These trinary slices will then be stacked up to form a 3-D distribution. This distribution will then be sampled in 3-D using our same hybrid sampling scheme used in emission studies. This will be done for each frame throughout the cardiac cycle. These results will then be filtered in space and time as described in 2.1. The centerline between endocardium and epicardium will be automatically determined so that it may be used in validating the myocardial shape as described in 2.1. Absolute thickness will be measured for each sampling radius in each 3-d distribution for all time intervals. The curves of absolute thickness as a function of time will be generated for each sample and submitted to the same FFT routine above to extract % thickening and phase. Validation: The thickening and phase will be compared in 20 patients undergoing both rest/stress sestamibi and MRI studies. The rms error for these two parameters will be determined. The accuracy of the emission technique in detecting thickening, its absence, and paradoxical thickening will be determined. Myocardial mass will also be determined from the MRI 3-D distribution by counting voxels and validated in the animal experiments.

3.2 Visualization of myocardial thickening.

Surface rendering. Models will be generated as described in 2.3 and 2.4 above. In the static model the tiles will represent either % SW thickening, phase or end-diastolic thickness (MRI). In the animated display the tiles will represent counts for the emission studies or thickness for the MRI studies. Conventional cine display of the beating slices along the short, horizontal and vertical long axis will be compared to this methodology to assess the extent, location and severity of abnormal thickening.

Volume rendering. For the emission studies a volume rendered model will be generated by using the thickening arrays to generate an "endocardial" wall from the surface model, i.e. the maximum thickening for each sample will be normalized to a particular absolute thickness away from the epicardial surface. Two methods will be explored to visualize wall thickness. The first approach is to display cross-sectional segments of the myocardium cut at any desired orientation. The second approach is to imbed the thickness information as an opacity factor which makes the walls translucent so that both the perfusion and wall thickness information are visualized simultaneously. Similar approaches will be used for volume-rendering the MRI data except that the absolute regional thickness will be used instead of using the relative thickening information. A final volume-rendered approach will be investigated which will show a combination of the emission and MRI data. In this approach the MRI data will be volume rendered using a gray-scale with the emission color-modulated count data aligned and superimposed.

PROJECT 4. UNIFIED QUANTIFICATION AND VISUALIZATION OF ANATOMIC AND PHYSIOLOGIC INFORMATION. This project is to continue to automate the registration of the 3-D coronary arterial tree onto the myocardial distributions and to quantify combined anatomic/physiologic parameters of myocardial dysfunction.

Method of procedure: The 3D coronary arterial tree will be registered onto one of the myocardial models using the methodology described in 4.1 below. The hypothesis is that the proximal length of the LAD and posterior descending branch (PDA) of the RCA arteries follow interventricular grooves which are easily identified from the perfusion sestamibi studies. Also the proximal length of the left circumflex (LCX) (where available such as MRI) follows the left atrioventricular groove. Registration will consist of superimposing the major coronary vessels on these grooves previously identified from the processed myocardial short axis slices (interventricular) and vertical long axis (atrioventricular). Once these two 3D distributions are merged into a single structure we will visualize them as an animated display using our modeling and rendering programs (projects 4.1 and 4.2) or they will be used to quantify parameters which depend on both the anatomic and physiologic variables such as: a) the extent and severity of stenotic lesions based on myocardial mass and perfusion (project 4.3) and b) the extent and severity of myocardium at jeopardy (project 4.4).

4.1 Automated registration and visualization of 3D coronary arterial tree on 3D myocardial perfusion distribution. After appropriate scaling, registration in 3D consists of a two-step process involving gross alignment and fine alignment for both imaging modalities, at the same portion of the cardiac cycle. (For single-frame myocardial studies the alignment will be assumed to be at end-diastole).
Gross alignment. This requires that the orientation of the long axis of the LV will remain the same with respect to both detectors frame of reference (e.g. patient facing up for both procedures). Presently the coronary vasculature is reconstructed in absolute space (in mm) with the isocenter of the angiographic device being the frame of reference. The nuclear scans generate a myocardium where the operator-selected long axis of the heart passes through its frame of reference. Although this is not the same frame of reference as the coronaries these reorientation programs provide in a file header the two angular degrees of freedom used for the reorientation. Using these two angles as well as the voxel dimensions the myocardial distributions are scaled and transformed to coincide with the frame of reference of the coronaries. All of these steps will be totally automated during this continuation and they will also be implemented for the MRI studies.
Automated fine alignment. This consists of registering, through rotations and translations, the appropriate coronary artery onto the known interventricular groove as identified from the myocardial slices (see Appendix 3.8). In both the pig model and in patients the proximal half of the LAD coronary trunk is fitted to fiducial marks representing the anterior longitudinal interventricular sulcus (groove) assigned from histogram equalized short axis slices. The LCX branch is then automatically registered based on its geometrical relationship to the LAD branch. Additional landmarks (such as the septum for the septal branches and the atrioventricular groove for the LCX) will be used to constrain the unification process as explained below. The proximal half of the PDA coronary trunk is independently fitted to the posterior sulcus (groove). Although initially all fittings were performed manually (interactively) using MAX, all results shown in this proposal were obtained using the following automated technique. Presently the operator assigns the following 4 fiducial marks to unify the left arterial tree: 1) the first point on the groove (groove1), 2) the first point on the LAD right after the left main (coro1), 3) a second point on the LAD which defines the LAD unification axis (coro2), and 4) the last point on the 1st diagonal (tip1). Note that due to the hierarchical nature of the file structure representing the vascular model (2) it will be straight forward to assign all but coro2 automatically. The automated process is initiated by translating groove1 and coro1 to the origin of the frame of reference, thus making the groove (heart) and the vasculature coincide. A point along the groove is determined (groove2) which makes the Euclidean distance between it and groove1 the same and the Euclidean distance between coro1 and coro2. At this point two axes have been defined, one for the arterial tree (coro1-coro2) and one for the groove/heart (groove1-groove2). Two rotations are then performed for the groove and for the coronary so both these axes align along the x axis. A third rotation is then performed on the coronary around the x axis until tip1 touches the surface of the myocardium. For additional mathematical detail see (21-Appendix 3.8). Thus the vasculature and myocardium are aligned. The arterial tree is then warped onto the myocardium by moving each of the vessel centerpoints which make up the vascular model along the myocardium's radius of sampling until it falls a vessel's radius above the myocardium. The magnitude of the move is called the warping distance for that sample. The alignment may then be improved by changing the location of coro2 or tip1 and iterating the above process. During this continuation we will implement an automated method which will iterate the above process, i.e. move coro2 along the vessel until the warping distance is minimized, then iterate by moving tip1 until the warping distance is further minimized. An user interface for picking coro2 (or any triplet) in 3-D will also be implemented to further expedite the registration procedure. A similar procedure is used for the PDA. During this continuation, we will also implement a correction on the warping algorithm to better use the "shape" of the myocardium as described from the vasculature. In this case the myocardium will be non-linearly warped until it coincides with the shape of the vasculature. Differences between shapes will be mathematically mitigated.

4.2 Automated registration and temporal visualization of 3D coronary arterial tree on 3D myocardial distribution. Registration and visualization will be performed as in 4.1 above but will be repeated for each of the 8 frames of the cardiac cycle tracking the manually assigned or automatically determined fiducial marks from the 1st frame. Animation will be done as explained in 2.4.

4.3 Quantification of the extent and severity of stenotic lesions based on myocardial mass and perfusion. Quantification will be performed on the patients and animals which have undergone angiography, perfusion tomography and MRI (for mass) after unification of all studies. This quantification will account for: a) myocardial mass probably hypoperfused due to the stenotic lesion (> 50% diameter narrowing or 75% lumen area reduction [>10% flow impairment])without using perfusion information and b) myocardial mass hypoperfused using the myocardial perfusion distribution.

a) The extent of myocardial mass (absolute and relative) involved by a stenotic lesion will be determined based on a volumetric model of the myocardium on which the reconstructed 3D coronaries are superimposed.

In general, the region distal to the stenotic vessel, not supplied by another vessel will be considered hypoperfused. In particular, the boundaries of the region will be determined as a "center line" between the stenotic vessel and all of its neighboring normal vessels. The proximal boundary of the hypoperfused region is defined by a plane perpendicular to the stenotic vessel, and passing through the stenosis. Once the region is defined, the mass corresponding to this region extracted from the MRI scan will be used to determine the extent of the stenosis. The severity of the stenosis will be calculated as the product of the extent of hypoperfused myocardium times a stenosis hypoperfused index (SHI) varying from 0 (normal) to 1 (100% occluded). The SHI will be determined according to the amount of flow impairment predicted for such a lesion, either in terms of % stenosis or according to the relation between the vessel's normal to stenotic absolute cross sectional areas.

b) The extent of the hypoperfused myocardial mass due to a stenotic lesion will also be determined using the 3D perfusion representation from the SPECT study. After appropriate processing and alignment to the coronary tree, the hypoperfused myocardial mass related to a stenosis will be determined as the mass corresponding to the abnormally perfused (below normal limits) blacked out region. The severity of the stenosis will be determined as in a above. These determinations will be compared to a above.

4.4 Quantification of the extent and severity of myocardium at jeopardy. The mass of the myocardium at jeopardy (MAJ) will be determined as follows: Mass MAJ = mass(Rev U St U AbTh), where Rev is the region determined to be an ischemic perfusion defect , St is the region determined in 4.3.a above from the stenosis location , AbTh is the region determined to thicken abnormally and U is the algebraic union of these regions. Usually all three regions would coincide and the region would be counted only once. The extent of MAJ will then be given as a percentage of the mass MAJ to the mass of the viable (total minus the infarcted) myocardium. The severity of MAJ is determined by multiplying the pixels which define the mass MAJ by a factor from 0 to 1 (obtained as the maximum severity of the perfusion defect, stenotic lesion or abnormally thickening wall) and dividing by the mass of the viable (total minus the infarcted) myocardium.

PROJECT 5. FURTHER VALIDATION OF QUANTIFICATION AND VISUALIZATION METHODOLOGY. The overall approach will be to use the animal and patient studies to measure how accurate the 3-D models are represented by each modality and how accurate these modalities can be unified (registered) onto one display.

5.1 Validations using the animal model. The aims of this subproject are to determine how accurately we can measure the following parameters. 1) the 3D model of the vasculature, 2) the 3D distribution of sestamibi, 3) the definition of the interventricular grooves from the SPECT studies, 4) the registration of the obstructed vessel onto the myocardium, 5) the registration of the SPECT myocardium onto the MR one, 6) the % mass hypoperfused (myocardium at jeopardy) by a combination of the MR and SPECT studies.

EXPERIMENTAL APPROACH: In-vivo experiment: The pigs will be premedicated with Ketamine (25mg/Kg) and Atropine (.02 mg/Kg) and then anesthetized with intravenous Nebutol (10-15mg/Kg). A cutdown will expose the femoral artery and the left coronary arteries will be cannulated under fluoroscopic guidance using suitable guiding catheters. Control perfusion experiment: During angiography a dose of 1.33 mCi of Tc-99m sestamibi will be injected into the left main and a separate dose of .66 mCi into the RCA. The animal's normal perfusion distribution will then imaged using gated SPECT. Intervention: After 10 half-lives of Tc-99m (60 hrs) the animal will be brought back. The animal will again be anesthetized and cannulated. An inflatable balloon catheter will be advanced into the LAD of 12 pigs (different locations) and the LCX (different locations) of another 12 pigs and the PDA of another 12. Four sets of simultaneous biplane angiographic studies will then be performed (two sets left tree image at different orientations and two right) by injecting X-ray contrast material while the balloon is deflated in order to obtain the normal coronary vasculature. The balloon will then be inflated to create a 100% occlusion for > 2 mins. During this period another biplane angiographic study will be performed to record the balloon position and to insure there is no distal flow present. During balloon occlusion, a dose of approximately 1.33 mCi of Tc-99m sestamibi will be injected into the left main, proximal to the balloon. A separate dose of .66 mCi will be injected into the RCA (also proximal to balloon when occluded). The animals will then be imaged using gated SPECT. For these animal experiments, we will record a 2nd scatter window and perform a transmission scan to compare results to our method of scatter and attenuation correction (103,104). No funding is requested for this comparison. Ex-vivo experiment: Upon completion of the acquisition, the pigs will be transported to the animal lab where they will be sacrificed using intravenous Euthanasia 5 solution (sodium pentobarbital, etc). The chest will then be opened. The heart will then be excised. A portion of the aorta and vena cava will be left intact for later clamping. The left and right ventricles will be filled with vinyl latex to give the heart a fixed shape. The site of occlusion will be identified by visually locating the distended portion of the vessel. A balloon catheter will

then be advanced to the same position, inflated, and a buffered solution of Dextran and monastral blue dye is injected at physiological pressures distal to the balloon to outline the region where sestamibi should be absent. After the catheter is removed the vessel will be ligated at the site of occlusion along with a point source of In-111 and MR contrast (water doped with Cu-sulfate, ~1gm/L) which will be used to record the error of the unification. The heart is then mounted on a plastic jig where there are three additional external point sources which will be used to measure the error of unifying the nuclear and MR study. The excised heart will then be imaged using dual energy SPECT (Tc-99m and In-111) and high-resolution MR (2mm in-plane resolution with 6mm contiguous slices). The coronary artery that was obstructed will be opacified with X-ray contrast material and imaged with biplane angiography. The heart is then returned to the animal lab where it is sliced perpendicular to their long axis in 6 mm thick slices. The coronaries are then highlighted with a color marker. Both sides of each slice will be imaged with a video camera for further digitization and analysis. The LV myocardium is then weighed. The stained portion of the myocardium is cut free from the surrounding myocardium and also weighed.

Analysis of angiographic data. 3D models of the in-vivo left and right vascular trees are reconstructed from two non-orthogonal projections and reprojected back to the original projections and to the other projections not used for the reconstruction. The rms distance between vessel centerlines and rms difference in vessel width will be determined for the error between the reprojected 3D model and the corresponding projections. The analysis will be repeated by reconstructing using all 4 acquired projections. This procedure will be repeated for the ex-vivo study. Accuracy of SPECT and MR myocardial registration. The 3D ex-vivo model of perfusion will be registered onto the 3D MR model using the interventricular grooves as a guide and using the Pelizarri algorithm as the final registration. The rms distance between the 3 external sources will be used as a measure of accuracy. The rms distance between the two sets of grooves will be used to determine the accuracy of the SPECT grooves. Note, the markers are not used for alignment, but to test the accuracy of the registration technique. Accuracy of unification of vasculature and myocardium. The 3D ex-vivo model of the vasculature will be registered onto the myocardium as described in 4.1. The rms distance between the centerline of the most distal point on the obstructed vessel and the myocardial marker will be used to measure the accuracy of the registration. This will be done for both the MR and perfusion myocardium. The in-vivo 4D (3D + time) vascular model will be registered onto the beating SPECT myocardial 3D model. The warping distance will be used as a parameter of registration accuracy. Accuracy of myocardium at jeopardy calculation. After the ex-vivo perfusion 3D model is registered onto the MR 3D model we will determine MAJ as per 4.4 using the mass from the abnormally perfused region and will compare it to similar calculations from a volumetric 3D model of the digitized slabs.

5.2 Validation using patient studies. The aims of this subproject are to determine how accurate we can: 1) label the vessel pairs by the knowledge based system as described in 1.2 to allow totally automated reconstruction and 2) measure the 3D model of the vasculature. 3) Define the clinical benefits of the approach. Methods. 140 Patients having both a standard biplane angiographic study and a standard myocardial perfusion study within a month of each other will form the basis of this study (3 patients/month plus the 16 already acquired). Patients intervened between procedures or patients with bypass grafts will be excluded. Acquisition and processing protocols are described in projects 1 and 2.

Analysis. Accuracy of automated reconstruction. Each angiographic study will be manually processed by an expert observer to draw the vessels' edges and to identify the corresponding vessel pairs from the biplane projections. The same projections are then used as input to the automatic reconstruction program. The 3D vascular model generated with manual assistance will be compared to the automatically reconstructed 3D model. The rms distance between vessel centerlines and rms difference in vessel widths will be determined as the error of the automated approach. In addition, the rms distance between vessel centerlines and rms difference in vessel widths will be determined for the error between the reprojected (automatic) 3D model and the corresponding projections. Accuracy and usefulness of unification. The 4D vascular models will be registered onto the temporal sequence of the 3D models of myocardial perfusion as described in project 4.1. The warping distance will be used as an indicator of the registration error. The sensitivity and specificity of the 3D perfusion model alone for localizing disease will be determined using the predetermined scheme established in (78). Using the unified model, the location and extent of the hypoperfused region as determined from the perfusion study will be compared to the location and extent of the myocardium at jeopardy from the stenotic vessel. We expect a better correlation with this latter approach since the predetermined approach does not allow for variations in vessel position. We will also correlate the combined myocardium at jeopardy from the unified model with the following parameters: 1st pass ejection fraction, exercise tolerance, stress EKG, survival and future myocardial infarction, in most patients in which this information will be available.